Nanoscale Research Letters

NANO EXPRESS Open Access

Phase Engineering for Highly Efficient Quasi-Two-Dimensional All-Inorganic Perovskite Light-Emitting Diodes via Adjusting the Ratio of Cs Cation

Xiaoqiang Xu[1,2], Zijun Wang[1], Junsheng Yu[1], Lu Li[1] and Xingwu Yan[2*]

Abstract

Quasi-two-dimensional (2D) perovskites have received intensive attention as a new class of luminescent materials owing to large exciton binding energy and high photoluminescence efficiency. However, there usually contains a mixture of phases in these materials, and excessive low-dimensional phase perovskite is harmful for luminescence efficiency owing to the strong exciton-phonon quenching at the room temperature. Herein, a simple and effective method is proposed to suppress the growth of low-dimensional phase components in quasi-2D perovskite film via carefully adjusting the molar ratio of cesium bromide (CsBr) and phenylpropylammonium bromide (PPABr). The device based on this optimized film has achieved a peak brightness of 2921 cd m^{-2} and peak current efficiency of 1.38 cd A^{-1}, far away higher than that of the pristine $CsPbBr_3$ device. This research proves a new way for modulating the phase composition in quasi-2D perovskites to fabricate highly efficient perovskite light-emitting diodes (PeLEDs).

Keywords: Perovskite light-emitting diodes, Quasi-2D, Phase engineering, Phenylpropylammonium

Introduction

Perovskite materials have aroused intensive research interests in thin-film light-emitting diodes owing to their exceptional optoelectronic properties, such as easily tunable emission wavelength [1, 2], high ambipolar charge mobility, facile solution processability, and low material cost [3–7]. But relatively low exciton binding energy and poor film-forming ability have resulted in inferior emission properties [8]. To circumvent these problems, many strategies have been adopted to boost the luminous efficiency in PeLEDs, such as composition modulating [9–12], interface engineering [13–16], nanocrystal pinning [17], solvent engineering [18–22], and polymer doping [23–25]. The external quantum efficiency (EQE) of the latest PeLEDs has been approaching 20%, nearly comparable to that of the current OLED [26, 27], which shows its great potentials for lighting and display applications.

Recently, quasi-2D perovskites, generally known as $L_2(CsPbX_3)_{n-1}PbX_4$, have become the research hot materials in PeLEDs owing to high photoluminescence quantum efficiency (PLQY) and significantly improved stability compared to three-dimensional (3D) perovskite [28–36]. In these materials, the introduced alkyl or phenyl ammonium cations cannot fill into the interspace of $[PbX_6]^{4-}$ octahedral because of large ionic radius, resulting in the formation of layered perovskite film with self-assembly multiple-quantum-wells structure via spin-coating. In the quasi-2D perovskite structure, excitons are limited in inorganic layers to recombination due to big difference of permittivity between the incorporated ammonium barrier layers (L) and inorganic $[PbX_6]^{4-}$ octahedral layer, resulting in enlarged exciton binding energy [28]. Compared to 3D counterparts, quasi-2D perovskite films possess higher PLQY, smoother film morphology, lower defect-state density, and better environmental stability, which are beneficial for light-emitting applications

* Correspondence: yan_xing_wu@126.com
[2]Research Institute for New Materials Technology, Chongqing University of Arts and Sciences, Chongqing 402160, People's Republic of China
Full list of author information is available at the end of the article

[29]. For example, phenylethylammonium (PEA) cations were firstly used in green emission ($PEA_2MA_{n-1}Pb_nBr_{3n+1}$) with the maximum EQE of 8.8% and brightness of 2935 cd m^{-2} [28]. *n*-Butylammonium (BA) were introduced into $MAPbBr_3$ perovskite precursor by Xiao et al. to obtain green PeLEDs with the EQE of 9.3% and a maximum brightness of 2900 cd m^{-2} [29]. Yang et al. reported the highly efficient green PeLEDs ($PEA_2FA_{n-1}Pb_nBr_{3n+1}$) with the EQE of 14.36% and peak luminance of 8779 cd m^{-2} based on perovskite films with $n = 3$ composition [34]. Recently, sky-blue PeLEDs with the peak brightness of 2480 cd m^{-2} were demonstrated based on $n = 3$ composition with double organic ammonium cations PEA and isopropyl ammonium (IPA) doping [35]. It has been demonstrated that the device based on quasi-2D perovskite with $n = 3$ composition can achieve high efficiency, but there exists a mixed phase in stoichiometric $n = 3$ composition perovskite [28, 34–37], which usually causes low emission efficiency. How to improve the phase purity in the quasi-2D perovskite remains a challenge.

In this work, by incorporating extra Cs cation into $n = 3$ composition perovskite precursor, efficient quasi-2D PeLEDs based on phenylpropylammonium bromide (PPABr) and $CsPbBr_3$ were fabricated. Compared to 3D $CsPbBr_3$ perovskite film, quasi-2D perovskite films exhibit full coverage, smaller grain size, and lower roughness. Moreover, the introduction of extra Cs cations in the precursor not only suppresses the formation of low-dimensional phase (little *n*-value-phase) with poor luminous efficiency, but also passivates the defect states in resulting quasi-2D perovskite film. Hence, the prepared perovskite films exhibit remarkable PL properties. By employing the resulting perovskite films as the emitting layer, quasi-2D PeLEDs with a peak brightness of 2921 cd m^{-2} and current efficiency of 1.38 cd A^{-1} were achieved, nearly threefold of that of the device based on $n = 3$ composition perovskite film.

Methods

Lead bromide ($PbBr_2$; Alfa Aesar, 99.999%); dimethyl sulfoxide (DMSO; 99.5% anhydrous, J&K Chemicals); poly(3,4-ethylenedioxythiophene):polystyrenesulfonate (PEDOT:PSS; Heraeus, VP AI4083); 1,3,5-tris(2-N-phenylbenzimidazolyl) benzene (TPBi; > 99.9%); cesium bromide (CsBr; 99.9%); and phenylpropylammonium bromide (PPABr; > 99.5%) were purchased from Xi'an Polymer Light Technology Corp. All materials were used as received without further purification. The perovskite precursor solutions were prepared by mixing PPABr, CsBr, and $PbBr_2$ in DMSO and stirred at 60 °C overnight with different molar ratios of 2:2:3, 2:3:3, 2:3.5:3, and 2:4:3, respectively. The concentration of $PbBr_2$ of every sample was kept constant in 0.15 M.

The ITO/glass substrates were ultrasonically cleaned in detergent, deionized water, acetone, and isopropanol in sequence for 20 min, respectively. After drying at 80 °C for 40 min, the substrates were treated in a UV-Ozone oven for 20 min prior to device fabrication. PEDOT: PSS (filtered by 0.45-μm PTFE syringe filter before deposition) was spin-coated onto cleaned substrates at 2900 rpm for 60 s and then baked at 150 °C for 20 min in the atmosphere. After that, all substrates were transferred into a nitrogen-filled glovebox. The as-obtained perovskite precursors were spin-coated onto substrates at 3000 rpm for 90 s and annealed at 90 °C for 15 min. The thickness of perovskite is about 70 nm. Next, TPBi (40 nm), LiF (1 nm), and Al (100 nm) were successively thermally deposited to complete the device in vacuum evaporation chamber under the basic pressure of 4×10^{-4} Pa. The active area of every PeLED is 0.11 cm^2.

The current density-luminance-voltage (*J-L-V*) characteristic curves were monitored via two programed Keithley 2400 measurement unit coupled to a calibrated silicon photodiode. Electroluminescence (EL) spectra were recorded with a Photo Research PR670 spectrometer. PeLED characterizations were conducted in a nitrogen-filled glovebox without encapsulation. The morphology of perovskite films was investigated employing a field-emission scanning electron microscope (FESEM; ZEISS GeminiSEM 300) and atomic force microscope (AFM; Agilent AFM 5500). Structure characterization of perovskite films was conducted using an X-ray diffraction (XRD; X'Pert PRO, PANalytical). Absorption spectra of perovskite films were measured with an Agilent Cary 5000 UV-Visible spectroscopy. The steady-state PL spectra and time-resolved PL (TRPL) decay curves were determined by employing a HITACHI F7000 and an Edinburgh FLS980 fluorescence spectrophotometer, respectively.

Results and Discussion

Perovskite Film Characterizations

The absorption spectra of perovskite films with different compositions are shown in Fig. 1a and b. From Fig. 1a, we can see $CsPbBr_3$ film shows an absorption peak near 517 nm and PPA2PbBr4 film shows typical absorption peak at 400 nm, which corresponds to the $n = 1$ and $n = \infty$ phase perovskite, respectively, indicating that 2D perovskite has strong quantum confinement effects [28]. For perovskite films with different content of Cs cations, they all exhibit multiple absorption peaks, indicating that there indeed are mixed phase compositions in the four perovskite films [8, 34]. For $n = 3$ composition perovskite

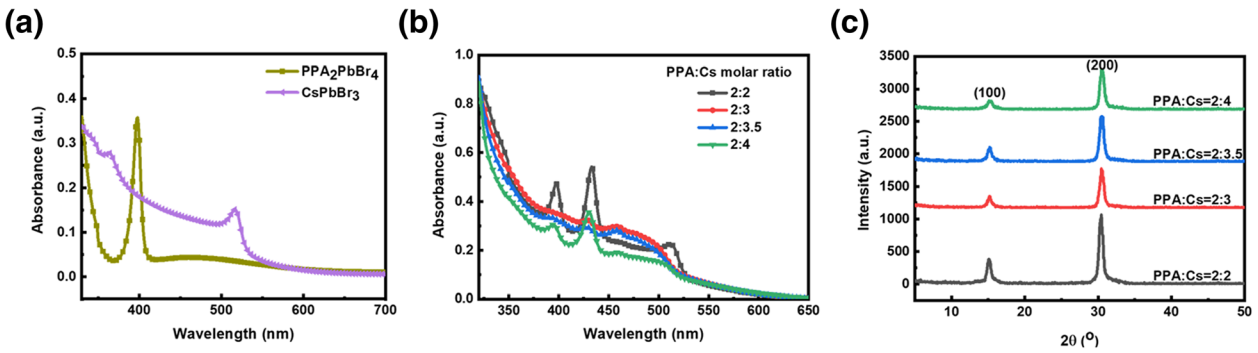

Fig. 1 Absorption spectra in thin films of **a** the 3D $CsPbBr_3$ and 2D PPA_2PbBr_4 perovskite, and **b** quasi-2D compounds with different molar ratios of PPA:Cs cations of 2:2, 2:3, 2:3.5, and 2:4. **c** XRD patterns of quasi-2D perovskite films with molar ratio of PPA:Cs cations of 2:2, 2:3, 2:3.5, and 2:4

film (2:2), the exciton absorption peak corresponding to low-*n*-value phase perovskite was high, which means there exit large low-*n*-value phase in the perovskite film. However, when increasing the relative content of Cs ratio in precursor solutions (2:3 and 2:3.5), the absorption peaks belonging to middle *n*-phase perovskite began to appear, which turn out that lots of low-*n*-value phase perovskites have been transformed to large-*n*-value phase. To investigate the influence of extra Cs cations on perovskite crystalline properties, the X-ray diffraction (XRD) measurements were adopted. All films exhibited only two prominent diffraction peaks at 15.15° and 30.45°, respectively, which can be assigned to the (100) and (200) crystalline planes of orthorhombic phase $CsPbBr_3$, indicating the preferential growth of perovskite crystallites, which is consistent with previous reports [30].

The morphological evolutions of perovskite thin films with different contents of Cs cations were recorded with SEM and AFM. From Figs. 2 and 3, we can see that pristine 3D $CsPbBr_3$ show a poor surface morphology with many voids and big root-mean-square (RMS) roughness, which may cause electric shunt paths. In contrary, when PPABr is used, the film coverage is remarkably enhanced, and grain size is decreased sharply. The RMS of the pure 3D $CsPbBr_3$ film is 9.49 nm, which is greatly

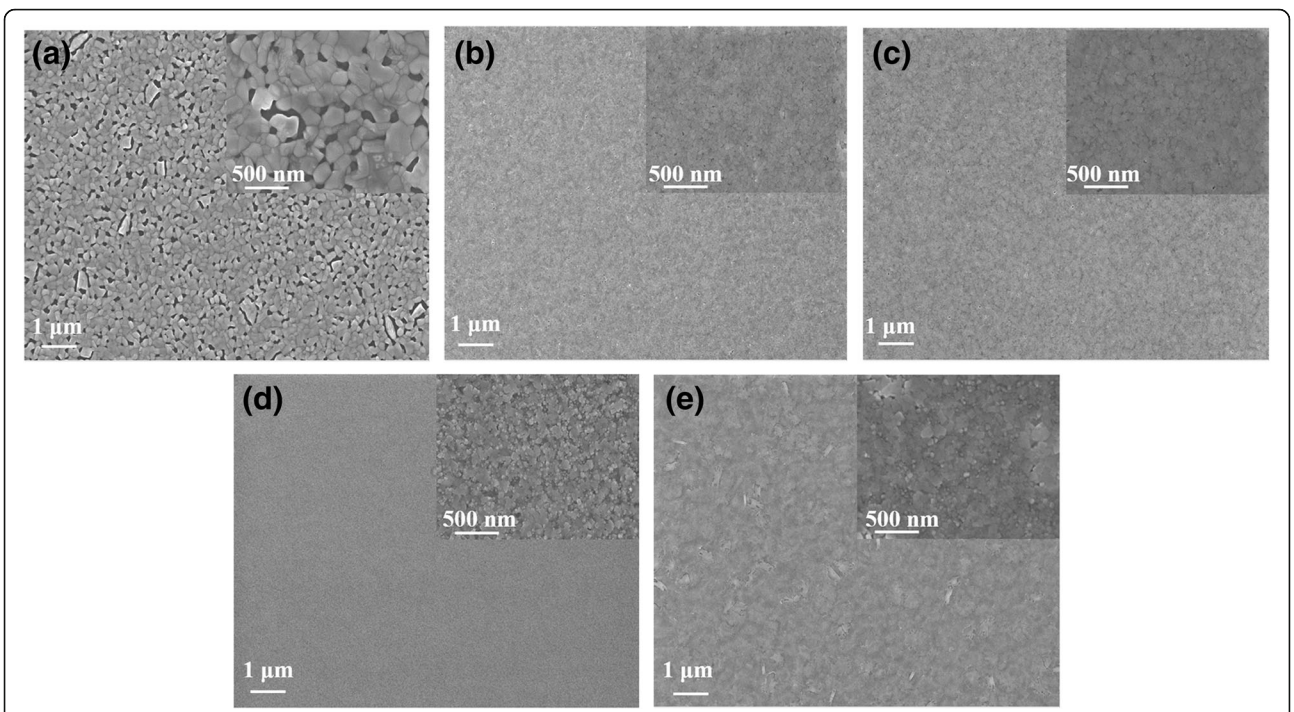

Fig. 2 SEM images of perovskite films with **a** 3D perovskite and quasi-2D perovskite based on PPA:Cs cations of **b** 2:2, **c** 2:3, **d** 2:3.5, and **e** 2:4; the insets show the magnified picture of corresponding SEM. **b** AFM topographies of corresponding perovskite films

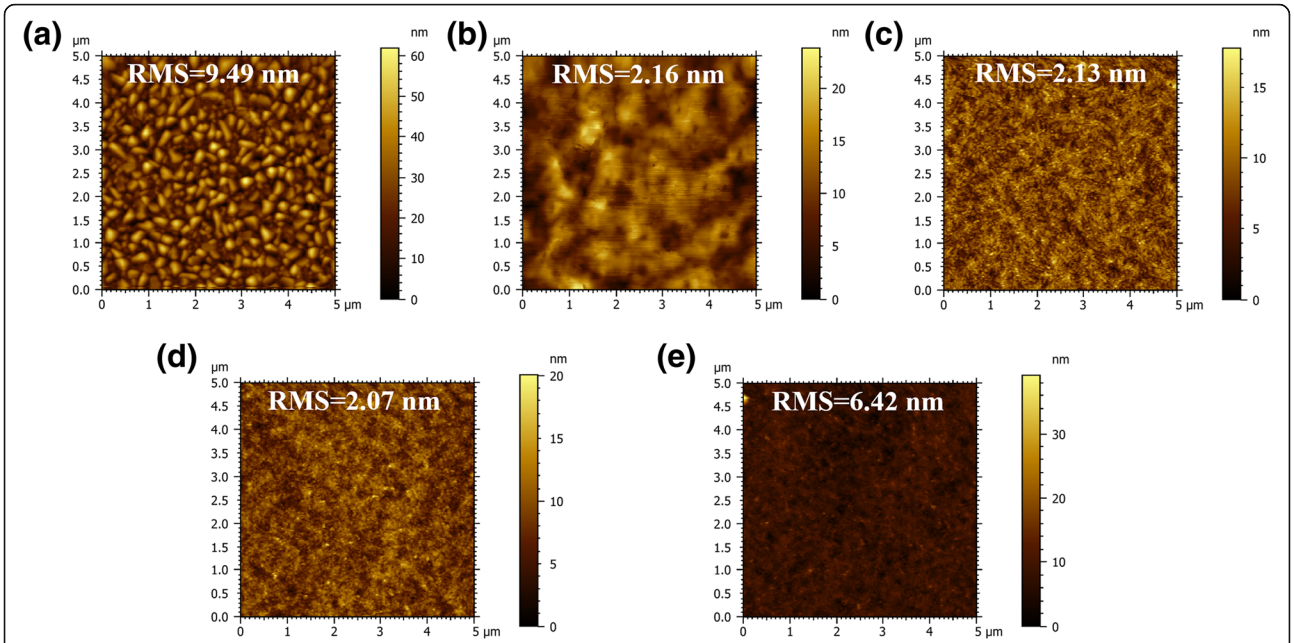

Fig. 3 **b** AFM topographies of corresponding perovskite films with **a** 3D perovskite and quasi-2D perovskite based on PPA:Cs cations of **b** 2:2, **c** 2:3, **d** 2:3.5, and **e** 2:4

decreased to 2.16 nm after the incorporation of PPABr (PPABr:CsBr = 2:2). When increasing the content of Cs cations to 2:3 and 2:3.5, the roughness remains at low levels. However, the surface became rough again when further increasing the Cs cation concentration to 2:4. These findings demonstrate that the incorporation of PPABr is indeed conducive to forming a compact and smooth thin film, and it could be found that incorporating Cs cations into precursor solution in an appropriate range has a little impact on perovskite thin film morphology.

Figure 4a exhibits the photoluminescence spectra of perovskite films with different molar ratios of PPA:Cs, which were measured to probe *n*-phase modulation in perovskite films. Obviously, photoluminescence emission peak gradually blueshifted from 524 nm for 3D $CsPbBr_3$ thin film to 517 nm for perovskite thin films of 2:2, indicating an incremental quantum confinement effect. When increasing the relative content of Cs cations, the PL spectra show a slight redshift. Meanwhile, the perovskite film with the PPA:Cs molar ratio of 2:3.5 shows the highest PL intensity under the same excitation condition. To gain deep insight into the effect of Cs content in the precursor solution on exciton properties of perovskite films, time-resolved photoluminescence (TRPL) decay curves of perovskite films were measured and displayed in Fig. 4b, which can be well fitted by tri-exponential expression (1) [38]:

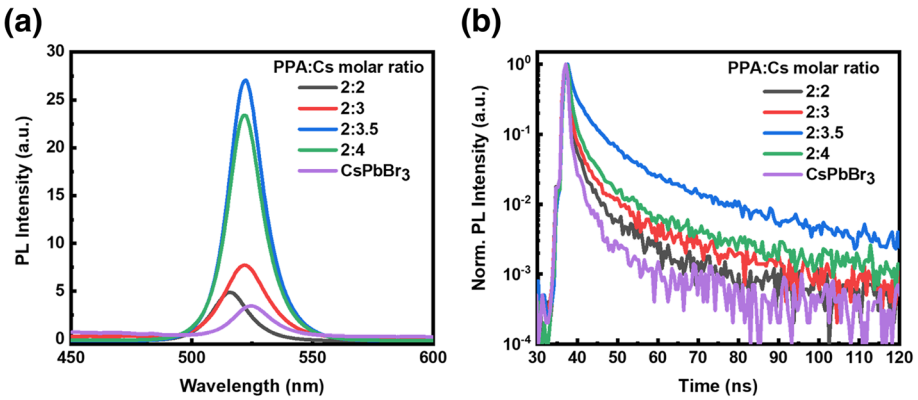

Fig. 4 **a** PL spectra and **b** normalized TRPL decay curves of perovskite films with different molar ratios of PPA:Cs

Table 1 Detailed fitted parameters of time-resolved photoluminescence decay curve

PPA:Cs	A_1 (%)	τ_1 (ns)	A_2 (%)	τ_2 (ns)	A_3 (%)	τ_3 (ns)	τ_{avg} (ns)
2:2	40.73	0.55	41.52	3.17	17.75	19.49	14.35
2:3	32.98	1.40	42.52	6.15	24.51	30.48	23.17
2:3.5	28.72	1.69	50.87	8.26	20.42	44.70	32.11
2:4	53.32	0.72	32.79	4.93	13.90	41.67	32.03
$CsPbBr_3$	76.64	0.32	18.24	2.17	5.12	12.56	7.02

$$I = A_1 e^{-\frac{t}{\tau_1}} + A_2 e^{-\frac{t}{\tau_2}} + A_3 e^{-\frac{t}{\tau_3}} \quad (1)$$

in which I represents the normalized PL intensity; A_1, A_2, and A_3 stand for the proportion of the components; and τ_1, τ_2, and τ_3 represent respective exciton lifetime for different carrier kinetic process. The average lifetime (τ_{avg}) is calculated in the following expression (2) [19]:

$$\tau_{avg} = \frac{A_1\tau_1^2 + A_2\tau_2^2 + A_3\tau_3^2}{A_1\tau_1 + A_2\tau_2 + A_3\tau_3} \quad (2)$$

where the τ_3 component is ascribed to radiative recombination process in perovskite grains and τ_1 and τ_2 correspond to two types of trap-assisted recombination. Table 1 summarizes the fitted parameters of the three-exponential fitting result of TRPL decays. The average time for a pristine 3D $CsPbBr_3$ sample is small (7.02 ns). But it is improved significantly by introducing PPA, which is attributed to greatly enlarged exciton binding energy [29]. And when increasing the Cs cation content in the precursor solution, the τ_{avg} of 2:3.5 shows the largest average lifetime of 32.11 ns, indicating that there is decreased defect-state density compared to perovskite films with other compositions, in combination with the similar surface morphology and absorption spectra. According to the above discussion, it can be concluded that appropriate Cs cations in perovskite precursor can impede the growth of the low-n-perovskite phase perovskite [37] and led to decreased trap density and prolonged carrier lifetime.

LED Device Fabrication

Employing abovementioned perovskite films as an emitting layer, perovskite LEDs (ITO/PEDOT: PSS/$PPA_2(CsPbBr_3)_{n-1}PbBr_4$/TPBi/LiF/Al) were fabricated, as shown in Figs. 5 and 6a and b. Figure 6c–e displays current density, luminance, and current efficiency as a function of voltage (*J-V*, *L-V*, and CE-*V*) characteristic curves for the devices with different molar ratios of PPA: Cs cations. It can be clearly seen that the incorporation of PPABr leads to the obvious decrease in leakage current under low applied voltages, demonstrating remarkably reduced shunting paths in perovskite film, in good agreement with the morphology characterization results mentioned above. As shown in Fig. 6d and e, the device with PPA:Cs molar ratio of 2:2 shows the significantly improved peak brightness of 1026 cd m^{-2} compared with that of 60 cd m^{-2} for 3D $CsPbBr_3$-based device, and the current efficiency improved from 0.01 to 0.80 cd A^{-1}. With further improvement in the Cs cations in the perovskite precursor solutions, the maximum luminance and current density got further improvements, of which the device with the PPA:Cs molar ratio of 2:3.5 exhibits the peak luminance of 2921 cd m^{-2}, which is nearly threefold improvement compared with that of the device with the PPA: Cs molar ratio of 2:2, and the current density increased to 1.38 cd A^{-1}. The electroluminescence spectra (Fig. 6e) of PeLEDs with different compositions all show slightly redshifted emission peaks compared to the corresponding PL peaks, which is consistent with previous reports [37, 38]. Concrete PeLED characterization results are summarized in Table 2. Significantly improved device performance could be ascribed to improved morphology and reduced proportion of low-dimensional phase perovskite resulting from the extra Cs cations.

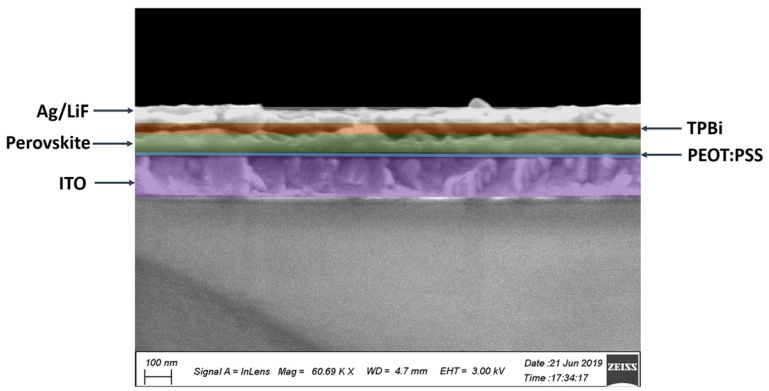

Fig. 5 Cross-sectional field-emission SEM of a quasi-2D PeLED

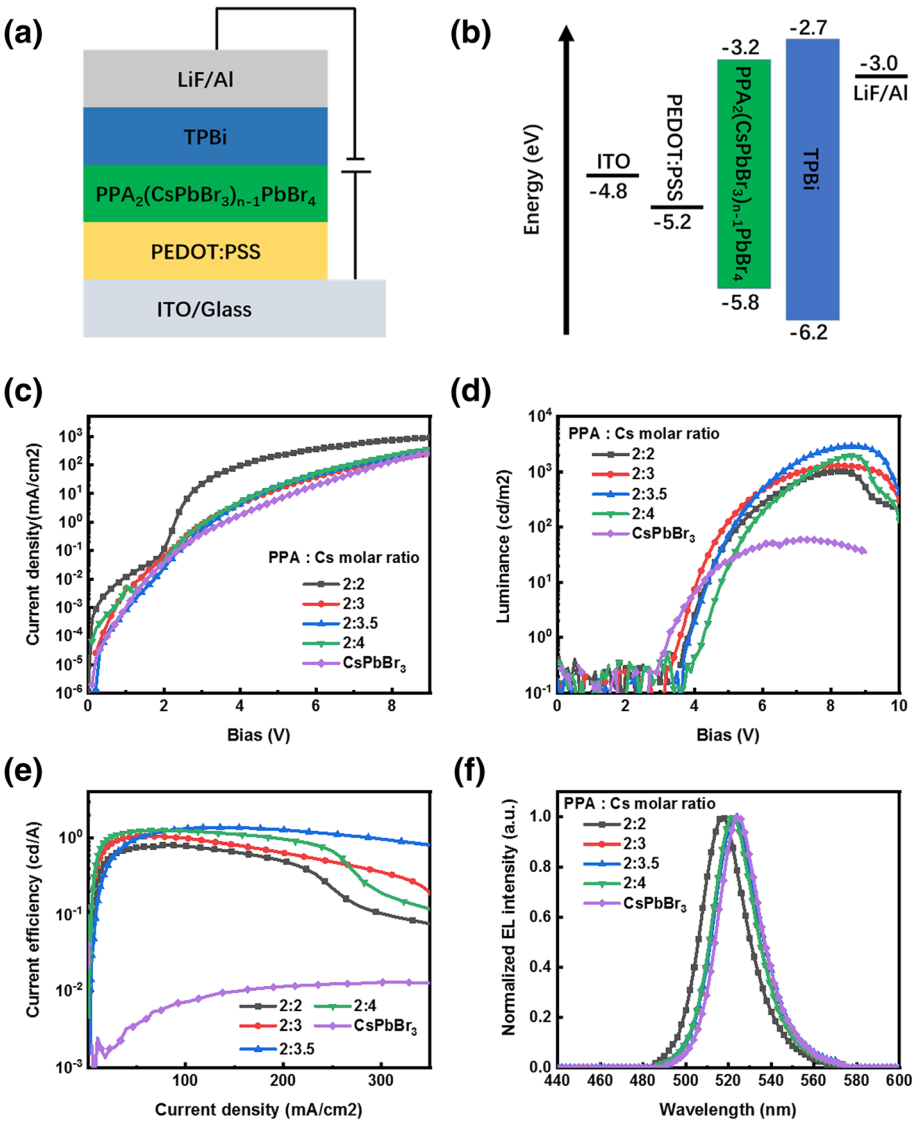

Fig. 6 **a** Schematic diagram of the device structure and **b** corresponding energy level for the PeLEDs. **c** Current density versus voltage curves (J-V), **d** luminance versus voltage (L-V), and **e** current efficiency versus voltage (CE-V) characteristic curves of PeLEDs based on different perovskite films. **f** Normalized EL spectra

Conclusions

In summary, a facile and efficient strategy to achieve high-performance perovskite LEDs via phase engineering has been developed. It is found that the introduction of organic spacer (PPABr) could remarkably reduce the domain size and increase the surface coverage of perovskite film. By further incorporating moderate cesium bromide into quasi-2D perovskite, the proportion of low-dimensional phase component in quasi-2D perovskite was significantly diminished, leading to a remarkably

Table 2 Summary of detailed PeLED performance parameters

PPA:Cs	$V_{turn\text{-}on}$ (V)	L_{max} (cd m^{-2})	CE_{max} (cd A^{-1})	EQE_{max} (%)	EL peak (nm)
2:2	3.8	1026	0.80	0.004	517.0
2:3	3.6	1289	1.05	0.006	522.4
2:3.5	3.8	2921	1.38	0.01	523.0
2:4	4.2	1944	1.25	0.007	522.2
$CsPbBr_3$	3.3	60	0.01	–	524.6

enhanced photoluminescence intensity and prolonged exciton lifetime. Hence, best performing PeLED based on the optimum Cs cation content shows a peak brightness of 2921 cd m^{-2} and a current efficiency of 1.38 cd A^{-1}, respectively. It is believed that this method may provide a guide for improving the emission efficiency of PeLEDs with quasi-2D perovskite film.

Abbreviations

2D: Two-dimensional; 3D: Three-dimensional; AFM: Atomic force microscope; CE-V: Current efficiency-voltage; CsBr: Cesium bromide; EQE: External quantum efficiency; FESEM: Field-emission scanning electron microscope; ITO: Indium tin oxide; J-V: Current density-voltage; L-V: Luminance-voltage; $PbBr_2$: Lead bromide; PeLEDs: Perovskite light-emitting diodes; PLQY: Photoluminescence quantum efficiency; PPABr: Phenylpropylammonium bromide; TRPL: Time-resolved photoluminescence; XRD: X-ray diffraction; τ_{avg}: Average lifetime

Acknowledgements

We thank the Research Institute for New Materials Technology, Chongqing University of Arts and Sciences, Chongqing.

Authors' Contributions

XX designed and carried out the experiments. ZW helped to analyze the data. XY, LL, and JY supervised this work. XX completed the manuscript. All authors read and approved the final manuscript.

Funding

This work was financially supported by the National Key Research and Development Program of China (Grant No. 2018YFB0407102), the Foundation for Innovation Research Groups of the National Natural Science Foundation of China (NSFC) (Grant No. 1361421002), the Foundation of the NSFC (Grant Nos: 61675041, 51503022, and 51703019), the Scientific and Technological Research Program of Chongqing Municipal Education Commission KJ1601126, and the Chongqing Science and Technology Commission (No.cstc2015jcyjA50036, No.cstc2016jcyjys 50001, and No.cstc2016jcyj0367).

Availability of Data and Materials

All datasets are presented in the main paper or in the additional supporting files.

Competing Interests

The authors declare that they have no competing interests and the mentioned received funding in our manuscript does not lead to any conflict of interests regarding the publication of this work.

Author details

[1]State Key Laboratory of Electronic Thin Films and Integrated Devices, School of Optoelectronic Science and Engineering, University of Electronic Science and Technology of China (UESTC), Chengdu 610054, People's Republic of China. [2]Research Institute for New Materials Technology, Chongqing University of Arts and Sciences, Chongqing 402160, People's Republic of China.

Received: 11 March 2019 Accepted: 7 July 2019
Published online: 27 July 2019

References

1. Zhang F, Zhong H, Chen C, Wu X, Hu X, Huang H, Han J, Zou B, Dong Y et al (2015) Brightly luminescent and color-tunable colloidal $CH_3NH_3PbX_3$ (X = Br, I, Cl) quantum dots: potential alternatives for display technology. ACS Nano. 9(4):4533–4542
2. Protesescu L, Yakunin S, Bodnarchuk MI, Krieg F, Caputo R, Hendon CH, Yang RX, Walsh A, Kovalenko MV et al (2015) Nanocrystals of cesium lead halide perovskites ($CsPbX_3$, X = Cl, Br, and I): novel optoelectronic materials showing bright emission with wide color gamut. Nano Lett. 15:3692–3696
3. Tan Z, Moghaddam RS, Lai ML, Docampo P, Higler R, Deschler F, Price M, Sadhanala A, Pazos LM, Credgington D, Hanusch F, Bein T, Snaith HJ, Friend RH et al (2014) Bright light-emitting diodes based on organometal halide perovskite. Nat Nano. 9:687–692
4. Yantara N, Bhaumik S, Yan F, Sabba D, Dewi HA, Mathews N, Boix PP, Demir HV, Mhaisalkar S et al (2015) Inorganic halide perovskites for efficient light-emitting diodes. J Phys Chem Lett. 6:4360–4364
5. Chen YC, Chou HL, Lin JC, Lee YC, Pao CW, Chen JL, Chang CC, Chi RY, Kuo TR, Lu CW, Wang DY (2019) Enhanced luminescence and stability of cesium lead halide perovskite $CsPbX_3$ nanocrystals by Cu^{2+}-assisted anion exchange reactions. J. Phys. Chem. C. 123:2353–2360
6. Behera RK, Adhikari SD, Dutta SK, Dutta A, Pradhan N (2018) Blue-emitting $CsPbCl_3$ nanocrystals: impact of surface passivation for unprecedented enhancement and loss of optical emission. J. Phys. Chem. Lett. 9:6884–6891
7. Tong Y, Fu M, Blate E, Huang H, Richter AF, Wang K, Muller-Buschbaum P, Bals S, Tamarat P, Lounis B, Feldmann J, Polavarapu L (2018) Chemical cutting of perovskite nanowires into single-photon emissive low-aspect-ratio $CsPbX_3$ (X=Cl, Br, I) Nanorods. Angew. Chem. Int. Edit. 57:16094–16098
8. Wang N, Cheng L, Ge R, Zhang S, Miao Y, Zou W, Yi C, Sun Y, Cao Y, Yang R, Wei Y, Guo Q, Ke Y, Yu M, Jin Y, Liu Y, Ding Q, Di D, Yang L, Xing G, Tian H, Jin C, Gao F, Friend RH, Wang J, Huang W et al (2016) Perovskite light-emitting diodes based on solution-processed self-organized multiple quantum wells. Nat Photonics. 10:699–704
9. Jin F, Zhao B, Chu B, Zhao H, Su Z, Li W, Zhu F et al (2018) Morphology control towards bright and stable inorganic halide perovskite light-emitting diodes. J Mater Chem C. 6:1573–1578
10. Cho H, Kim JS, Wolf C, Kim Y, Yun HJ, Jeong S, Sadhanala A, Venugopalan V, Choi JW, Lee C, Friend RH, Lee T et al (2018) High-efficiency polycrystalline perovskite light-emitting diodes based on mixed cations. ACS Nano. 12:2883–2892
11. Zhang X, Wang W, Xu B, Liu S, Dai H, Bian D, Chen S, Wang K, Sun XW et al (2017) Thin film perovskite light-emitting diode based on $CsPbBr_3$ powders and interfacial engineering. Nano Energy. 37:40–45
12. Wei Z, Perumal A, Su R, Sushant S, Xing J, Zhang Q, Tan ST, Demir HV, Xiong Q et al (2016) Solution-processed highly bright and durable cesium lead halide perovskite light-emitting diodes. Nanoscale. 8:18021
13. Cho H, Wolf C, Kim JS, Yun HJ, Bae JS, Kim H, Heo JM, Ahn S, Lee TW et al (2017) High-efficiency solution-processed inorganic metal halide perovskite light-emitting diodes. Adv Mater. 29:1700579
14. Wang Z, Li Z, Zhou D, Yu J et al (2017) Low turn-on voltage perovskite light-emitting diodes with methanol treated PEDOT: PSS as hole transport layer. Appl Phys Lett. 111:233304
15. Zhang L, Yang X, Jiang Q, Wang P, Yin Z, Zhang X, Tan H, Yang YM, Wei M, Sutherland BR, Sargent EH, You J et al (2017) Ultra-bright and highly efficient inorganic based perovskite light-emitting diodes. Nat Commun. 8:15640
16. Song L, Guo X, Hu Y, Lv Y, Lin J, Fan Y, Zhang N, Liu X et al (2018) Improved performance of $CsPbBr_3$ perovskite light-emitting devices by both boundary and interface defects passivation. Nanoscale. 10:18315–18322
17. Cho H, Jeong SH, Park MH, Kim YH, Wolf C, Lee CL, Heo JH, Sadhanala A, Myoung N, Yoo S, Im SH, Friend RH, Lee TW et al (2015) Overcoming the electroluminescence efficiency limitations of perovskite light-emitting diodes. Science. 350:1222–1225
18. Gao Z, Zheng Y, Zhao D, Yu J et al (2018) Spin-coated $CH_3NH_3PbBr_3$ film consisting of micron-scale single crystals assisted with a benzophenone crystallizing agent and its application in perovskite light-emitting diodes. Nanomaterials. 8:787
19. Wang Z, Huai B, Yang G, Wu M, Yu J et al (2018) High-performance perovskite light-emitting diodes realized by isopropyl alcohol as green anti-solvent. J. Lumin. 204:110–115
20. Yuan S, Wang Z, Zhuo M, Tian Q, Jin Y, Liao L et al (2018) Self-assembled high quality $CsPbBr_3$ quantum dot films toward highly efficient light-emitting diodes. ACS Nano. 12:9541–9548
21. Lee S, Park JH, Nam YS, Lee BR, Zhao B, Di Nuzzo D, Jung ED, Jeon H, Kim J, Jeong HY, Friend RH, Song MH et al (2018) Growth of nanosized single crystals for efficient perovskite light-emitting diodes. ACS Nano. 12:3417–3423
22. Han D, Imran M, Zhang M, Chang S, Wu X, Zhang X, Tang J, Wang M, Ali S, Li X, Yu G, Han J, Wang L, Zou B, Zhong H et al (2018) Efficient light-emitting diodes based on in situ fabricated $FAPbBr_3$ nanocrystals: the enhancing role of the ligand-assisted reprecipitation process. ACS Nano. 12:8808–8816
23. Ling Y, Tian Y, Wang X, Wang JC, Knox JM, Perez-Orive F, Du Y, Tan L, Hanson K, Ma B, Gao H et al (2016) Enhanced optical and electrical

properties of polymer-assisted all-inorganic perovskites for light-emitting diodes. Adv Mater. 28:8983–8989
24. Song L, Guo X, Hu Y, Lv Y, Lin J, Liu Z, Fan Y, Liu X et al (2017) Efficient inorganic perovskite light-emitting diodes with polyethylene glycol passivated ultrathin $CsPbBr_3$ films. J. Phys. Chem. Lett. 8:4148–4154
25. Li J, Shan X, Bade SGR, Geske T, Jiang Q, Yang X, Yu Z et al (2016) Single-layer halide perovskite light-emitting diodes with sub-band gap turn-on voltage and high brightness. J. Phys. Chem. Lett. 7:4059–4066
26. Lin K, Xing J, Quan LN, de Arquer FPG, Gong X, Lu J, Xie L, Zhao W, Zhang D, Yan C, Li W, Liu X, Lu Y, Kirman J, Sargent EH, Xiong Q, Wei Z et al (2018) Perovskite light-emitting diodes with external quantum efficiency exceeding 20 per cent. Nature. 562:245–248
27. Cao Y, Wang N, Tian H, Guo J, Wei Y, Chen H, Miao Y, Zou W, Pan K, He Y, Cao H, Ke Y, Xu M, Wang Y, Yang M, Du K, Fu Z, Kong D, Dai D, Jin Y, Li G, Li H, Peng Q, Wang J, Huang W et al (2018) Perovskite light-emitting diodes based on spontaneously formed submicrometre-scale structures. Nature. 562:249–253
28. Yuan M, Quan LN, Comin R, Walters G, Sabatini R, Voznyy O, Hoogland S, Zhao Y, Beauregard EM, Kanjanaboos P, Lu Z, Kim DH, Sargent EH et al (2016) Perovskite energy funnels for efficient light-emitting diodes. Nat. Nano. 11:872–877
29. Xiao Z, Kerner RA, Zhao L, Tran NL, Lee KM, Koh T, Scholes GD, Rand BP et al (2017) Efficient perovskite light-emitting diodes featuring nanometre-sized crystallites. Nat. Photonics. 11:108–115
30. Si J, Liu Y, He Z, Du H, Du K, Chen D, Li J, Xu M, Tian H, He H, Di D, Lin C, Cheng Y, Wang J, Jin Y et al (2017) Efficient and high-color-purity light-emitting diodes based on in situ grown films of $CsPbX_3$ (X = Br, I) nanoplates with controlled thicknesses. ACS Nano. 11:11100–11107
31. Zou W, Li R, Zhang S, Liu Y, Wang N, Cao Y, Miao, Y, Xu M, Guo Q, Di D, Zhang L, Yi C, Gao F, Friend RH, Wang J, Huang W, et al. Minimizing efficiency roll-off in high-brightness perovskite light-emitting diodes. Nat. Commun. 2018;9:608.
32. Wang Z, Wang F, Sun W, Ni R, Hu S, Liu J, Zhang B, Alsaed A, Hayat T, Tan Z et al (2018) Manipulating the trade-off between quantum yield and electrical conductivity for high-brightness quasi-2D perovskite light-emitting diodes. Adv. Funct. Mater. 28(47):1804187
33. Yantara N, Bruno A, Iqbal A, Jamaludin NF, Soci C, Mhaisalkar S, Mathews N et al (2018) Designing efficient energy funneling kinetics in Ruddlesden-Popper perovskites for high-performance light-emitting diodes. Adv. Mater. 30:1800818
34. Yang X, Zhang X, Deng J, Chu Z, Jiang Q, Meng J, Wang P, Zhang L, Yin Z, You J et al (2018) Efficient green light-emitting diodes based on quasi-two-dimensional composition and phase engineered perovskite with surface passivation. Nat. Commun. 9:570
35. Xing J, Zhao Y, Askerka M, Quan LN, Gong X, Zhao W, Zhao J, Tan H, Long G, Gao L, Yang Z, Voznyy O, Tang J, Lu Z, Xiong Q, Sargent EH et al (2018) Color-stable highly luminescent sky-blue perovskite light-emitting diodes. Nat. Commun. 9:3541
36. Chang YH, Lin JC, Chen YC, Kuo TR, Wang DY (2018) Facile synthesis of two-dimensional Ruddlesden–Popper perovskite quantum dots with fine-tunable optical properties. Nanoscale Res. Lett. 13:247
37. Wu T, Yang Y, Zou Y, Wang Y, Wu C, Han Y, Song T, Zhang Q, Gao X, Sun B et al (2018) Nanoplatelet modulation in 2D/3D perovskite targeting efficient light-emitting diodes. Nanoscale. 10:19322–19329
38. Wang J, Song C, He Z, Mai C, Xie G, Mu L, Cun Y, Li J, Wang J, Peng J, Cao Y et al (2018) All-solution-processed pure formamidinium-based perovskite light-emitting diodes. Adv Mater. 30:1804137

Publisher's Note